This journal is © The Royal Society of Chemistry 2014

Theory of the nsOCT

It is well known that the object's structure can be described using 3D function, which is usually called the scattering potential:

$$U(\mathbf{r}) = \frac{1}{4\pi} k_0^2 \left[n^2(\mathbf{r}) - 1 \right] \tag{1}$$

or its Fourier transform:

$$F(\mathbf{K}) = \int U(\mathbf{r}) e^{-i\mathbf{K}\cdot\mathbf{r}} d^3 r \tag{2}$$

where $k_0 = \frac{2\pi}{\lambda_0}$, n – refractive index, , ***K*** - scattering vector. If ***r*** is large enough, then

$$\mathbf{K} = \frac{2\pi n}{\lambda}(\mathbf{s} - \mathbf{s_0}) \tag{3}$$

s, $\mathbf{s}_0$ are unit vectors of scattered and illumination waves (Fig.1a). In Cartesian coordinates ***K*** can be also written as

$$\mathbf{K} = 2\pi(\nu_x \mathbf{i} + \nu_y \mathbf{j} + \nu_z \mathbf{k}) \tag{4}$$

where ν_x, ν_y and ν_z – spatial frequencies along Cartesian coordinates.

We restrict our consideration to first Born approximation and do not show the dependence on time frequency. According to the this approximation in the scalar theory of scattering, if the object is illuminated by a monochromatic plane wave, the complex amplitude of the scattered wave at a given wavelength in the far zone for a given direction depends entirely on only one Fourier component (one spatial frequency) of the 3D scattering potential, labelled by the vector ***K***. At a constant illumination angle, the end points of each vector Fourier component of the 3D scattering potential corresponds to a point on Ewald's sphere with radius $R = n/\lambda$.

If the object is illuminated by a plane wave with a certain spectral bandwidth, then, at a fixed illumination angle (Fig. 1a), the spatial frequencies distribution in K-space can be illustrated as multiple Ewald's spheres with different diameters. The example of such spheres for object illuminated along optical axis z for n=1, depending on the wavelength, is presented in Fig. 1b.

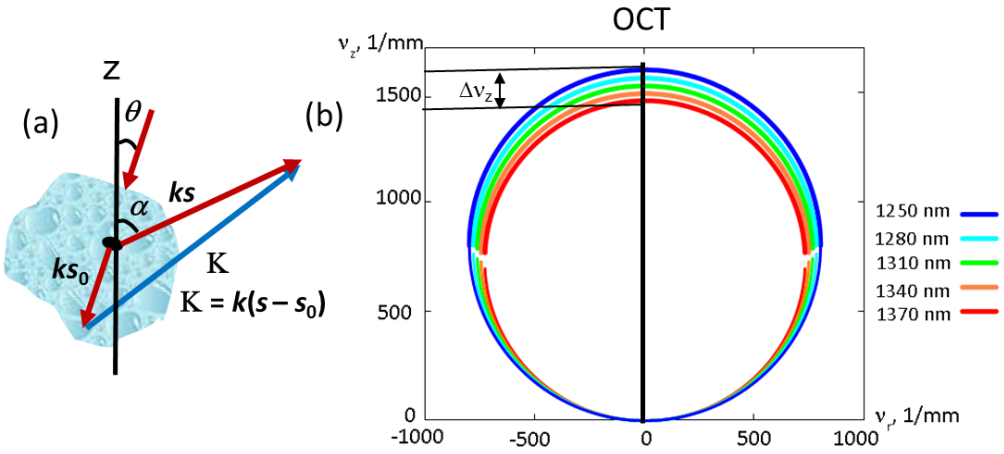

Fig. 1. (a) – Schematic of object illumination and collection; (b) – spatial frequency representation in K-space depending on wavelength.

The relations between spatial frequencies and wavelength can be written as

$$\nu_x = n(\sin\alpha - \sin\theta)\cos\phi/\lambda, \quad \nu_y = n(\sin\alpha - \sin\theta)\sin\phi/\lambda \tag{5}$$

This journal is © The Royal Society of Chemistry 2014

$$v_z = n\left(\cos\theta + \cos\alpha\right)/\lambda \,, \tag{6}$$

where n is the refractive index, θ is illumination angle, α is the scattering angle, and φ is the azimuthal angle (Fig. 1).

If we measure the scattered field (the complex amplitudes of the Fourier components) for all possible wavelengths, directions of illumination and scattering, then we could synthesize the 3D Fourier transform of the scattering potential. After that the scattering potential could be reconstructed as 3D inverse Fourier transform

$$U(\mathbf{r}) = \frac{1}{(2\pi)^3}\int F(\mathbf{K}) e^{-i\mathbf{K}\mathbf{r}} d^3K \,, \tag{7}$$

But even if spatial frequencies will be captured for all possible directions of illumination and scattering, we still will have limited range of spatial frequencies, the scattering potential will be reconstructed under low-pass filtered approximation and the best possible resolution is about half of wavelength. In conventional optical diffraction tomography the collected range of spatial frequencies is further limited by optical system. During the inverse Fourier transform to reconstruct the axial profile, the spatial information is integrated and, as a result, the resolution and sensitivity are reduced.

From Fig. 1 and Eq. (6) it can be seen that within moderate scattering angle α there is one to one correspondence between axial spatial frequency and wavelength. A spectral encoding of spatial frequency (SESF) approach uses this to encode axial spatial frequency through spectral diversity, translate it from Fourier domain into the image domain as a wavelength and map to each voxel of the 2D image.

OCT is one dimensional solution of the optical inverse scattering problem, where the Fourier components are collected along axial direction only (black line in Fig. 1b). Image formation in Fourier domain OCT (FDOCT) is based on a modification of the original formalism for the one-dimensional problem. In FDOCT each wavelength in collected spectrum corresponds to one axial spatial frequency (Fig. 1b) and so the axial component of the 3D scattering potential can be reconstructed via simplified Eq. (7), as 1D inverse Fourier transform. The axial spatial frequency range is

$$\Delta\nu_z = \frac{2n\Delta\lambda}{\lambda_1\lambda_2} \,, \tag{8}$$

where $\Delta\lambda = \lambda_2 - \lambda_1$ is the spectral range.

The axial spatial resolution of the FDOCT is limited by the range of axial spatial frequencies and can be calculated using formula:

$$R_{zOCT} = \frac{2\ln(2)\lambda_c{}^2}{n\pi\Delta\lambda} \,, \tag{9}$$

where λ_c - central wavelength. So to improve the axial resolution it is necessary to increase the spectral range $\Delta\lambda$.

Instead of straightforward way to improve the resolution and sensitivity of the OCT to structural changes by increasing the spectral range, we use different approach to probe the nanostructure, which we called nsOCT. Equation (6) for 1D OCT case can be rewritten as

$$v_z = \frac{2n}{\lambda}, \text{ and } H_z = \frac{1}{v_z} \tag{10}$$

To realize nsOCT we first convert the collected complex amplitudes of the spectrum to complex amplitudes of axial spatial frequencies according to (10). The complex spectrum of axial spatial frequencies can be decomposed into multiple sub-bands. We can also divide the object space into multiple volumes of interest (VOI) and calculate the energy contribution E_m of the ℓ_{th} spatial frequency sub-band to the spatial period profile of the m_{th} VOI at $H_{z\ell}$ as

$$I_m(H_{zl}) = \int_{V_m} \left|U_{m,l}(\mathbf{r})\right|^2 d\mathbf{r} \,, \tag{11}$$

where V_m represents the integration volume of the m_{th} VOI, and $U_{m,\ell}(\boldsymbol{r})$ is the inverse Fourier relation given by

$$\left|U_{m,l}(\mathbf{r})\right| = \frac{1}{(2\pi)^3}\int_{k_l} F(\mathbf{K})e^{i2\pi\mathbf{K}\cdot\mathbf{r}_m}d\mathbf{K}\,, \tag{12}$$

where $\boldsymbol{r}_m$ indicates that the contribution of the ℓ_{th} spatial frequency sub-band is considered only for the m_{th} VOI. By computing the energy contribution $I_m(H_{z\ell})$ for all the spatial periods $H_{z\ell}$, calculated using Eq. (10), we obtain axial spatial period profile for the m_{th} VOI. Using this procedure the axial spatial period profiles can be reconstructed for each voxel of the 3D image.

The signal processing flow chart for conventional FDOCT and nsOCT is presented in Fig. 2.

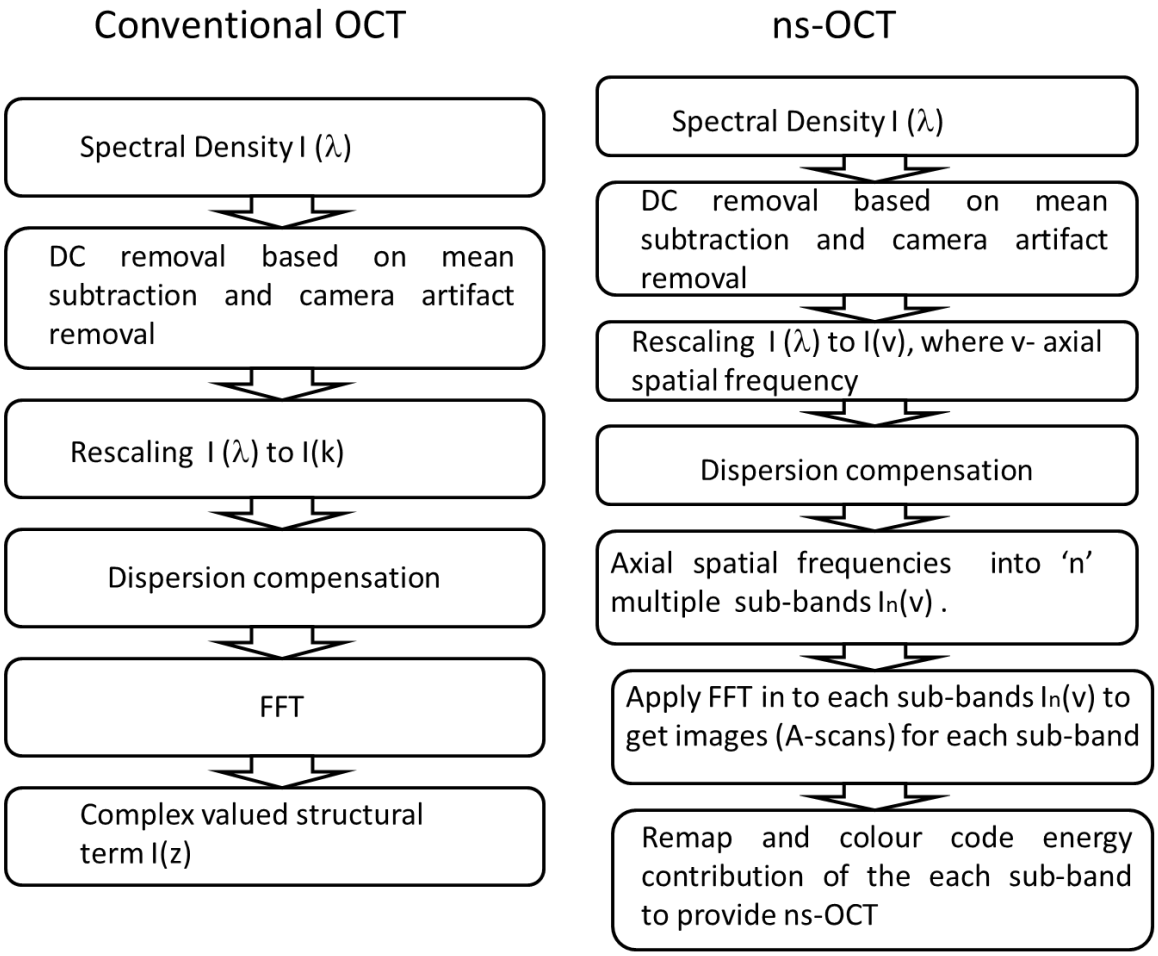

Fig. 2. The signal processing flow chart for conventional FDOCT and nsOCT.

Due to Fourier relation between **K**-space and object-space, the axial sampling interval in **K**-space controls the axial extent of the object. So the width of each sub-band will determine the axial size of the VOI within the object and the number of the sub-bands will determine the number of points for reconstruction of the axial spatial period profiles.

The smallest axial size of the VOI (axial voxel size) for given spatial frequency range $\Delta\nu_{zl}$ within ℓ_{th} sub-band can be defined as

$$\Delta z = \frac{1}{2\Delta\nu_{zl}}\,, \tag{13}$$

The smallest lateral size of the VOI is intrinsically defined by the diffraction-limited lateral resolution of the reconstructed 3D object. Submicron local structure can be visualized as corresponding spatial period profiles and nanoscale structural alterations within each voxel can be detected.

The smallest change in axial spatial period δH_z that the nsOCT can detect is defined as the sensitivity. The theoretical sensitivity to structural changes can be estimated by formula:

This journal is © The Royal Society of Chemistry 2014

$$\delta H_z = \frac{\delta\lambda}{2n}, \tag{14}$$

where δλ is the accuracy of the wavelength determination. One can estimate that if we measure the wavelength with accuracy 1 nm, then the theoretical sensitivity to structural changes is about 0.5 nm in air.

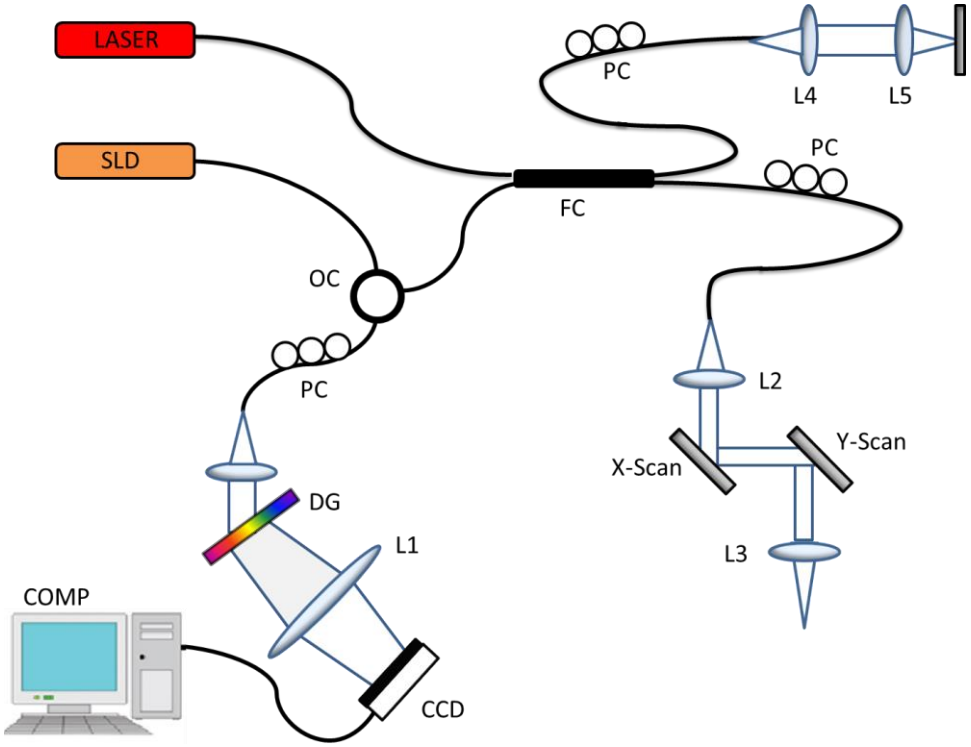

Fig. 3. SD-OCT setup for realization nsOCT.

The nsOCT was realized using full range SD-OCT setup presented in Fig. 3. A broadband 1310 nm superluminescent diode with bandwidth of 83 nm (SLD, Dense Light, Singapore) was coupled into the interferometer, via an optical coupler. The HeNe laser was used for system alignment.The spectrometer consisted of a 50 mm focal length collimator, a 1145 lines/mm transmitting grating, an achromatic lens with a 100 mm focal length and a 14-bit, 1024 pixels InGaAs line scan camera (SU1024LDH2, Goodrich Ltd. USA) with a maximum acquisition rate of 91 kHz. This spectrometer setup had a spectral resolution of 0.1432 nm, which gave a maximum imaging range of ~6 mm (in air). The frame rate for B-scan was 50 Hz. The measured axial imaging resolution of the system was ~ 12 µm in air (~9.2 µm in human skin). The sample arm consists of a pair of galvanometric driven mirrors and an objective lens with 50 mm diameter (NA=0.03) which provided a lateral resolution of ~ 30 µm. The measured sensitivity of the system was ~105 dB near the zero-delay line. The sensitivity drop off of the system was ~20 dB at a depth range ± 3 mm. The measured axial imaging resolution of the system was ~ 12 µm in air and a lateral resolution was ~ 30 µm.

NSOCT images were formed as maps of the maximal spatial periods for each voxel. According to presented theoretical analysis the uncertainty in spatial periods determination for NA= 0.03 objective lens was less than 1 nm. We used the voxel size in NSOCT images 30 µm x 30 µm x 50 µm. The spatial interval to reconstruct profiles of the axial spatial periods was 4 nm.